JOURNAL OF OPTOELECTRONICS AND ADVANCED MATERIALS, Vol. 11, No. 6, June 2009, p. 820 - 825

Study of the third-order nonlinear optical properties of nano-crystalline porous silicon using a simplified Bruggeman formalism

T. BAZARU*, V. I. VLAD, A. PETRIS, P. S. GHEORGHE
National Institute for Lasers, Plasma and Radiation Physics, Dept. of Lasers, R-077125 Bucharest - Magurele, Romania

In this paper, we simplify and apply optical modelling of Bruggeman-type nano-composites, for calculation of the effective optical linear and nonlinear properties of nano-structured silicon, in particular of nano-porous silicon. We used laser excitation with photon energy close to the estimated band-gap energy of nano-porous silicon, looking for important optical nonlinearities at low intensity levels. This regime is non-perturbative for the nano-structured sample and we observe pure optoelectronic effects in np-Si. The effective refractive index and effective third-order nonlinear susceptibility, calculated with our simplified formulae, and the corresponding measured parameters in our experiments are in good agreement.

(Received June 19, 2009; accepted June 22, 2009)

Keywords: Bruggeman model, Nano-porous silicon, Intensity scan, Reflection Z-Scan

1. Introduction

The nonlinear optical properties of nano-composites represent a topic of interest for photonics, because there is the hope that composite materials could display an enhanced and controllable nonlinear optical behaviour for photonic devices [1,2]. The nano-crystalline porous silicon (np-Si) can be considered as a particular example of nano-composite.

A number of authors studied the optical nonlinearities of nano-structured Si measured by transmission Z-Scan method [3-7]. Henari et al. [3] have been obtained, for porous Si, $\chi^{(3)} = 7.74\times10^{-9}$ esu, at $\lambda = 665$ nm ($I_0 = 1.6\times10^{8}$ W/cm^2). Vijayalakshmi et al. [4,5] have been reported the optical nonlinearities for silicon nanoclusters on quartz substrates, at $\lambda = 355$ nm and 532 nm. They estimated that linear refractive index for Si nanoclusters is $n_0 = 1.5$ and got the experimental values for third-order nonlinear susceptibility as $\chi^{(3)} = 2.28\times10^{-5}$ esu (at $\lambda = 355$ nm) [4] and $\mathrm{Re}\{\chi^{(3)}\} = (-1.33 \pm 0.33)\times10^{-3}$ esu (at $\lambda = 532$ nm, $I_0 = 0.03$ MW/cm^2) [5]. Lettieri et al. [6] have been reported the experimental values of below-gap nonlinear refractive index (n_2) for different wavelengths. They have been considered that the linear refractive index of porous Si is $n_0 = 1.9$ ($\lambda = 633$ nm) and the experimental values for nonlinear refractive index are $n_2 = (-5 \pm 1.3)\times10^{-9}$ esu (at $\lambda = 860$ nm, $I_0 = (1.4 \pm 0.1)\times10^{12}$ W/m^2), $n_2 = (-3.9 \pm 0.6)\times10^{-9}$ esu (at $\lambda = 900$ nm, $I_0 = (4.1 \pm 0.4)\times10^{12}$ W/m^2) and $n_2 = (-6.6 \pm 1.2)\times10^{-10}$ esu (at $\lambda = 1064$ nm, $I_0 = (3.5 \pm 0.4)\times10^{13}$ W/m^2). K. S. Bindra [7] has been estimated that nonlinear refractive index is $\gamma = 2.4\times10^{-15}$ cm^2/W (at $\lambda = 1064$ nm, $I_0 = 3.5$ GW/cm^2).

An important aim of this paper is to explain linear and third-order nonlinear optical properties of nano-porous silicon by using Bruggeman model [1,8,9], as this nano-composite is very close to Bruggeman geometry. The nano-porous silicon is a network of air pores (holes) within an interconnected silicon matrix. The sizes of Si structures can vary from a few nano-meters to a few microns depending on the conditions of formation and the characteristics of the silicon.

In order to use more easily Bruggeman formalism, we are derived a simple, but accurate, approximative formulae for the dependences of effective linear refractive index (n_{eff}) and for the third-order effective nonlinear susceptibility ($\chi_{eff}^{(3)}$) on Si volume fill fraction (for np-Si).

In our study, we are investigating optical nonlinearity of np-Si using a laser excitation with photon energy close to the estimated band-gap energy, at $\lambda = 633$ nm ($h\nu_l \approx 1.96$ eV), looking for important third-order optical nonlinearities in nano-composites at low laser intensity levels. At these intensity levels, the nano-structures of np-Si are not disturbed by thermal or other effects, so that pure optoelectronic effects can be studied. For measuring $\chi_{eff}^{(3)}$, we have used the intensity scan (I-Scan) [10] and reflection Z-Scan (RZ-Scan) methods [11-13]. We are comparing $\chi_{eff}^{(3)}$, predicted by Bruggeman model, with the experimental values of $\chi_{nPS}^{(3)}$ obtained by the intensity scan and reflection Z-Scan methods and we are showing that the data predicted by our simplified Bruggeman formulae are closer to our I-Scan experimental data (for np-Si).

2. Structural and linear optical properties of investigated nano-crystalline porous silicon

In order to measure the nonlinear optical parameters of np-Si, we need to know several linear properties of our samples. So, we studied firstly some structural and linear optical properties of our np-Si samples by using Atomic

Force Microscopy (AFM), photoluminescence and reflectivity measurements.

In most of the cases, the porous silicon is realized by electrochemical anodization (in particular, electrochemical etching) of bulk silicon in hydrofluoric acid (HF). The investigated nano-porous Si samples were prepared by this method and a uniform layer of porous silicon was formed by etching. The porosity and the thickness of the layer can be controlled by the current density, the duration of etching and the HF concentration [1,14-16]. Our samples were aged for more than one year.

Using an Atomic Force Microscope from Omicron Nanotechnology, we have obtained information about structure of the np-Si sample surface and sizes of nano-structures up to ~ 40 nm (Fig. 1). From these data, one can derive the volume fill fraction of our np-Si samples, which is approx. 0.18.

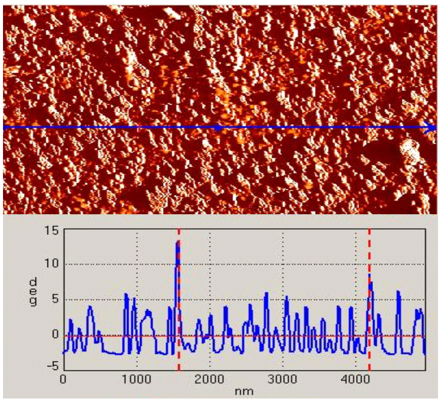

a

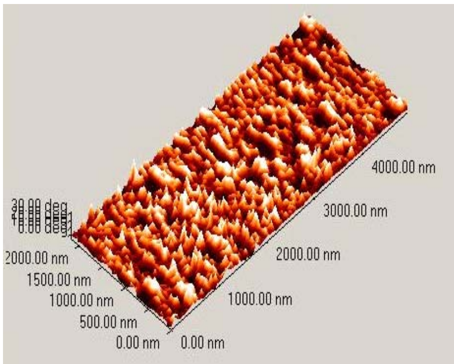

b

Fig. 1. AFM images of np-Si sample; (a) 2D image of np-Si layer and (b) 3D image of np-Si layer

Photoluminescence (PL) properties of np-Si layer were observed and measured with the experimental setup presented in Fig. 2. In order to study the PL characteristics of np-Si sample, we have used different excitation sources: a pulsed Nitrogen laser (λ = 337 nm, pulse duration t_p = 4 ns, pulse energy < 1mJ), the third harmonic of a pulsed Nd:YAG laser (λ = 355 nm, pulse duration t_p = 3 ns, maximum pulse energy 20 mJ) and a c.w. laser diode (λ = 466 nm). The excitation light beam was collimated and filtered (to select the desired wavelengths only). The luminescence light emitted by the np-Si sample was transmitted by an optical fiber to a measurement chain (monochromator, photomultiplier and oscilloscope), connected to a computer for data acquisition and processing.

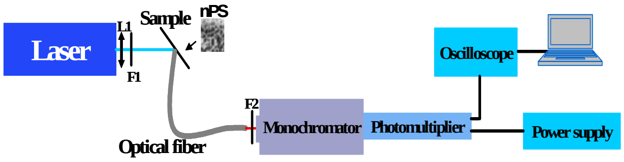

Fig. 2. Photoluminescence experimental setup

Using these three excitation sources (337 nm, 355 nm and 466 nm), we obtained the PL spectra that are presented in Fig. 3a-c.

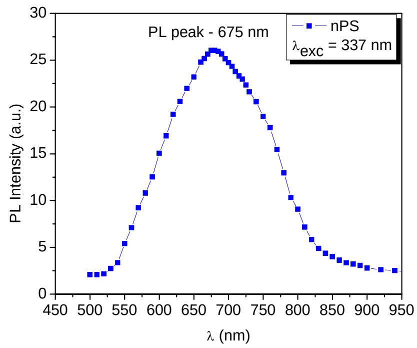

a

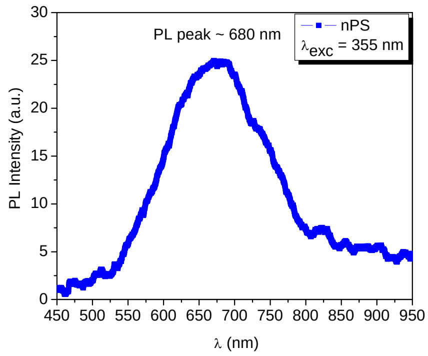

b

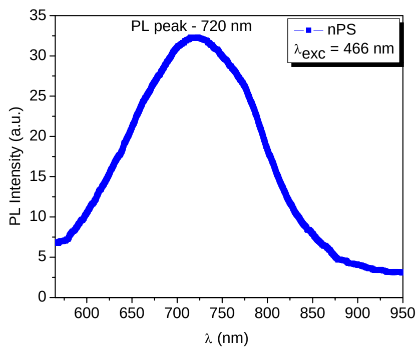

c

Fig. 3. PL spectra of the nano-porous Si excited with various wavelengths: (a) 337 nm, (b) 355 nm, (c) 466 nm.

These PL spectra show that the wavelengths of PL maxima are dependent on excitation wavelengths (Fig. 4). Increasing the excitation wavelength, the PL peak is obtained at higher wavelength. In order to make a better presentation of this dependence, we have introduced also a result obtained previously by Inanc et al. [16] for PL maximum, at 750 nm, when exciting the sample with light at 532 nm. From Fig. 4 we can see that this dependence is linear, which could be explained by the fact that, at short excitation wavelengths, all np-Si structures absorb the light, while at higher excitation wavelengths, the larger structures absorb preferentially. This result is in good agreement with that presented by Kux et al. [17].

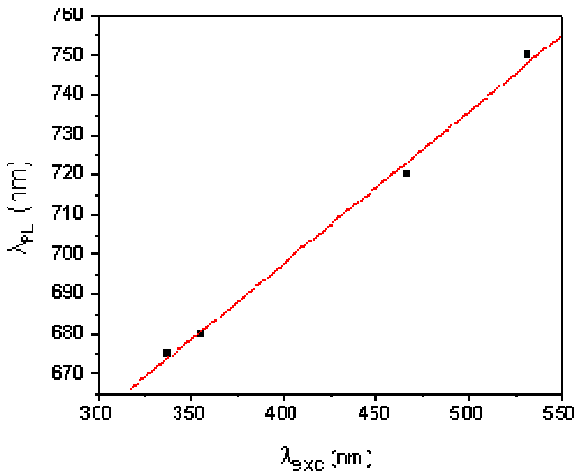

Fig. 4. Experimental dependence of wavelength of PL peak versus excitation wavelength (continuous line is theoretical fit of the experimental data)

Due to the size distribution of the np-Si structures inside the sample, is not possible to define a unique band gap. According Kux et al. [17], Calcott [18] and Lettieri et al. [19], a good approximation of the band gap is about 0.2 eV above PL peak energy. For our samples, we have estimated $E_g \sim 2$ eV.

3. Linear and nonlinear optical properties of np-Si described by Bruggeman model

The properties of porous silicon can be described by Bruggeman geometry [1], because consists of two randomly intermixed components and the dimensions of the Si nano-structures are much smaller than the excitation light wavelength. In general, the Bruggeman model can provide theoretical estimations for the effective linear dielectric constant and for the nonlinear optical properties of nano-composites, including np-Si. According to Bruggeman model, the effective linear dielectric constant of np-Si layer can be described by the following equation [1,8,9]:

$$f_{Si} \cdot \frac{\varepsilon_{Si} - \varepsilon_{eff}}{\varepsilon_{Si} + 2\varepsilon_{eff}} + f_{air} \cdot \frac{\varepsilon_{air} - \varepsilon_{eff}}{\varepsilon_{air} + 2\varepsilon_{eff}} = 0, \tag{1}$$

where f_{Si} and f_{air} are the volume fill fractions of components (Si and air), ε_{Si} and ε_{air} are the dielectric constants of Si and embedded medium (air), ε_{eff} is effective linear dielectric constant of np-Si layer. From Eq. (1), we have obtained explicitly $\varepsilon_{eff} = F(\varepsilon_{Si}, f_{Si})$:

$$\varepsilon_{eff} = \frac{1}{4}\left[2 - 3f_{Si} + \varepsilon_{Si}(3f_{Si} - 1) + \sqrt{8\varepsilon_{Si} + [2 - 3f_{Si} + \varepsilon_{Si}(3f_{Si} - 1)]^2}\right] \tag{2}$$

and the effective linear refractive index as:

$$n_{eff} = \sqrt{\varepsilon_{eff}}. \tag{3}$$

Calculating the effective refractive index with Eqs. (2) and (3), we observed that its dependence on the volume fill fraction is, in a good approximation, linear (for np-Si, at $\lambda = 532$ nm and $\lambda = 633$ nm) and we have derived the following simplified dependencies (Fig. 5):

$$\begin{aligned} n_{eff} &\approx 3.52 \cdot f_{Si} + 0.68 \quad , \quad for \quad \lambda = 532\,nm \\ n_{eff} &\approx 3.19 \cdot f_{Si} + 0.74 \quad , \quad for \quad \lambda = 633\,nm \end{aligned} \tag{4}$$

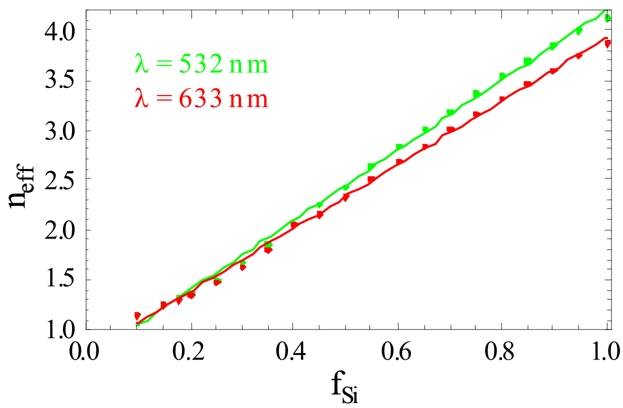

Fig. 5. Dependence of n_{eff} of np-Si versus f_{Si} for $\lambda = 532$ nm si $\lambda = 633$ nm (the dots - calculated n_{eff} for different f_{Si}, the lines - linear fits using Eqs. (4))

For $f_{Si} = 0.18$, Eq. (4) leads to $n_{eff} \approx 1.31$, (at $\lambda = 633$ nm), which is in a good agreement with the corresponding value provided by the reflectivity measurements, $n_{eff} = 1.303$.

In these measurements (Fig. 6), we used a He-Ne laser ($\lambda = 633$ nm) beam at near-normal incidence. The experimental data, collected in different positions of the np-Si sample, were averaged in order to obtain a good estimation of the intensity reflectivity of the sample. Using a Fresnel-type relation between this average reflectivity and the effective refractive index, we have found $n_{eff} \approx 1.303$ for our np-Si sample, with $f_{Si} = 0.18$.

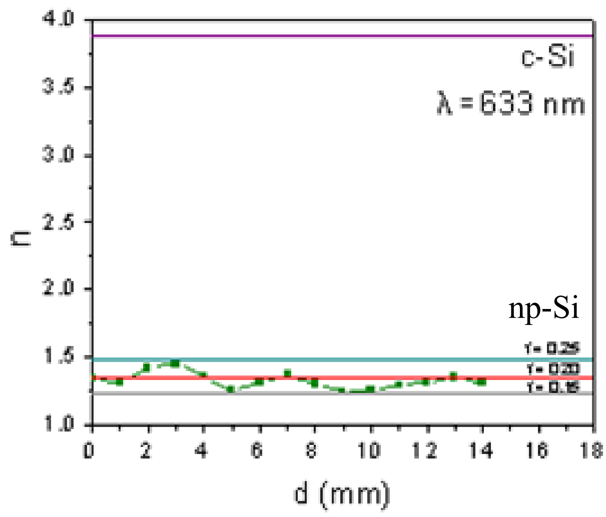

Fig. 6. Reflectivity data of np-Si sample vs. measurement position on the sample. In our case, f_{Si} = 0.18 and the average effective linear refractive index, $n_{eff} \approx 1.303$ (λ = 633 nm).

The nonlinear optical properties of a Bruggeman structure can be described by a statistical theory based on the assumption that the electric field within each component is uniform. This theory predicts that there is possible to obtain a small contribution of the nonlinearity to the nonlinear optical response. The effective nonlinear susceptibility can be determined with the formula derived by Boyd et al. [8, 9]:

$$\chi_{eff}^{(3)} = \sum_i \frac{1}{f_i} \left| \frac{\partial \varepsilon_{eff}}{\partial \varepsilon_i} \right| \left(\frac{\partial \varepsilon_{eff}}{\partial \varepsilon_i} \right) \chi_i^{(3)} \tag{5}$$

In the case of our np-Si sample, we have only one nonlinear component, i.e. silicon, because the air is linear at the laser intensity range used in our experiments. Consequently, Eq. (5) becomes:

$$\frac{\chi_{eff}^{(3)}}{\chi_{Si}^{(3)}} = \frac{1}{f_{Si}} \left(\frac{\partial \varepsilon_{eff}}{\partial \varepsilon_{Si}} \right)^2 = \frac{1}{f_{Si}} \left[\frac{1}{4} \left(3f_{Si} - 1 + \frac{2 - 9f_{Si}(f_{Si}-1) + \varepsilon_{Si}(1-3f_{Si})^2}{\sqrt{8\varepsilon_{Si} + (2 - 3f_{Si} + \varepsilon_{Si}(3f_{Si}-1))^2}} \right) \right]^2 \tag{6}$$

Using Eq. (6), we found a simple approximative quadratic dependence of the np-Si effective nonlinear third-order susceptibility on the Si volume fill fraction (at λ = 633 nm):

$$\frac{\chi_{eff}^{(3)}}{\chi_{Si}^{(3)}} \approx 1.48 \cdot f_{Si}^2 - 0.48 \cdot f_{Si}\,. \tag{7}$$

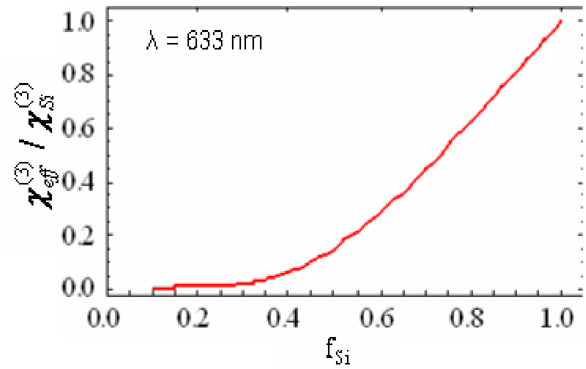

Fig. 7. Theoretical predictions of our simplified Bruggeman formula (7) for $\chi_{eff}^{(3)}$ plotted as a function of f_{Si}

Fig. 7 shows the quadratic increase of $\chi_{eff}^{(3)}$ with f_{Si}, which correctly tends to 1, when $f_{Si} \to 1$ (although this formalism is more accurate for low f_{Si}).

4. Third-order nonlinearity experimental investigation by intensity scan and reflection Z-Scan methods

Theoretical prediction for the third-order effective optical nonlinearity, $\chi_{eff}^{(3)}$, obtained with simplified Bruggeman formula (7) was experimentally verified by I-Scan method [10] and open-aperture RZ-Scan method [11-13].

The experimental setup is presented in Fig. 9, for both I-Scan and RZ-Scan methods. In the open-aperture RZ-Scan method, the investigated sample is moving along the incident beam direction, passing through the focal plane of a focusing lens and the reflected signal is measured by a measurement chain consisting of photo-detector, oscilloscope and PC. In the I-Scan method, the investigated sample is placed at approximately a Rayleigh length behind the focal plane of the lens and the laser intensity is varied. The samples are irradiated by a focused c.w. Gaussian beam (He-Ne laser, λ = 633 nm).

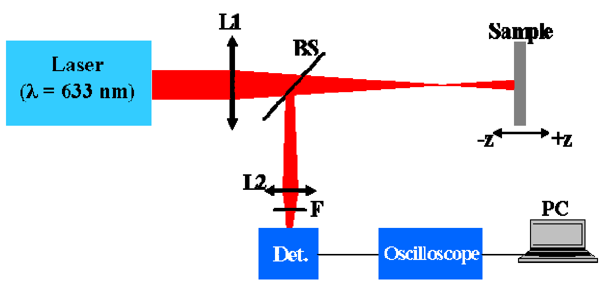

Fig. 8. I-Scan and RZ-Scan experimental setup: c.w. laser (He-Ne or diode) (λ = 633 nm), L1, L2- lenses (f_1= 12.5 cm, f_2 = 10 cm), BS – beam-splitter, F – neutral filter, Det. – photo-detector. For RZ-Scan, the sample is moved with a mobile platform, controlled by a driver.

In RZ-Scan method, the open-aperture nonlinear normalized reflection (the ratio between the power reflected by the sample with and without the nonlinear effect) was derived as [13]:

$$R(z) \approx 1 + \frac{2 \cdot \chi_{eff}^{(3)} \cdot I_0}{19 \cdot n_{eff}^2 \left(n_{eff}^2 - 1\right) \cdot \left[1 + \left(z / z_R\right)^2\right]}, \qquad (8)$$

where: I_0 is the laser beam intensity in the focus (I_0 = 6.35×10^6 W/m^2), $z_R = \pi w_0^2 / \lambda$ is the Rayleigh length of the beam (in this setup, z_R = 1.2 cm) and w_0 is the beam waist. In the case of measurements on bulk Si sample, $n_{eff} = n_{0Si}$ and $\chi_{eff}^{(3)} = \chi_{Si}^{(3)}$.

For I-Scan method, we can use the same formalism as in the case of RZ-Scan, which leads to the nonlinear normalized reflection dependence on intensity:

$$R(I) \approx 1 + \frac{2 \cdot \chi_{eff}^{(3)} \cdot I}{19 \cdot n_{eff}^2 \left(n_{eff}^2 - 1\right) \cdot \left[1 + \left(z_1 / z_R\right)^2\right]}, \qquad (9)$$

where: z_1 is the distance behind the focus (z_1 = 1 cm), where the sample is placed, and I is the laser beam intensity at distance z_1 from the focus.

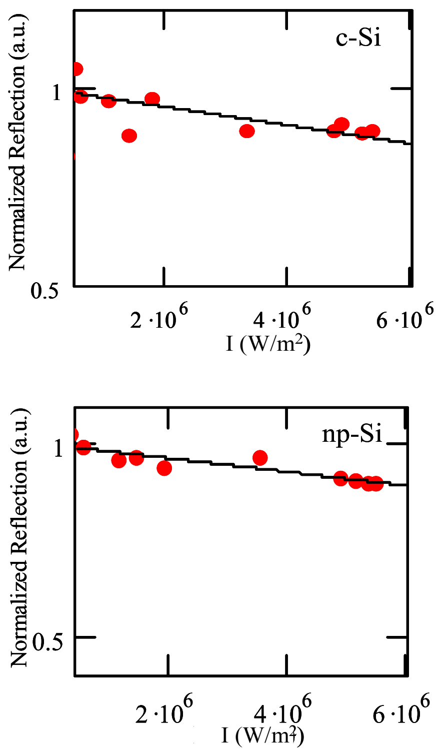

Fig. 9. I-Scan experimental data of $\chi_{Si}^{(3)}$ si $\chi_{eff}^{(3)}$

For a good verification of the Bruggeman theoretical prediction, we experimentally measured the third-order nonlinear optical susceptibilities of a crystalline Si wafer (c-Si) (n_{0Si} = 3.873) and a np-Si sample (n_{eff} = 1.303). The I-Scan experimental data presented in Fig. 9 are fitted with formula (9) and the values of third-order optical nonlinear susceptibilities of c-Si and np-Si samples, $\chi_{Si}^{(3)}$ and $\chi_{eff}^{(3)}$, are obtained. In Fig. 10, we show the RZ-Scan experimental data, which are fitted with the dependence from Eq. (8) in order to get $\chi_{Si}^{(3)}$ and $\chi_{eff}^{(3)}$.

In Fig. 11, we present the theoretical predictions of $\chi_{eff}^{(3)}$ given by our simplified Bruggeman formula (7) and the experimental results obtained with I-Scan and RZ-Scan methods, for a sample with f_{Si} = 0.18.

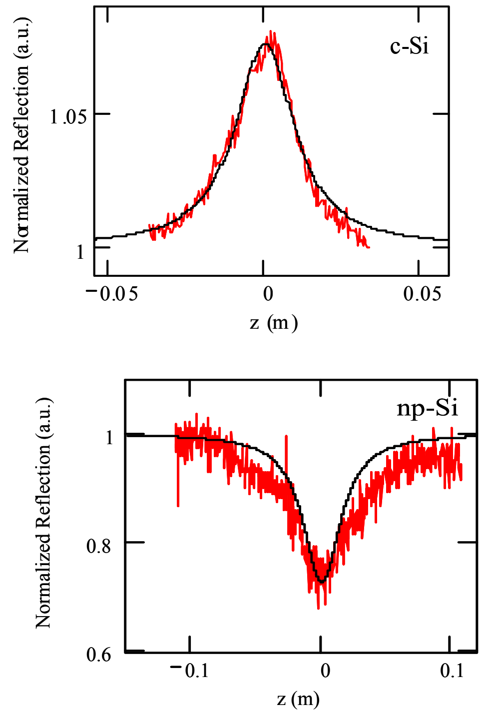

Fig. 10. RZ-Scan experimental data of $\chi_{Si}^{(3)}$ si $\chi_{eff}^{(3)}$

When compared with the RZ-Scan experimental data, the I-Scan measured optical nonlinearities are in better agreement with the data predicted by our simplified formula. The theoretical prediction calculated with (7) is $\left(\chi_{eff}^{(3)} / \chi_{Si}^{(3)}\right) = 1.78\times10^{-3}$.

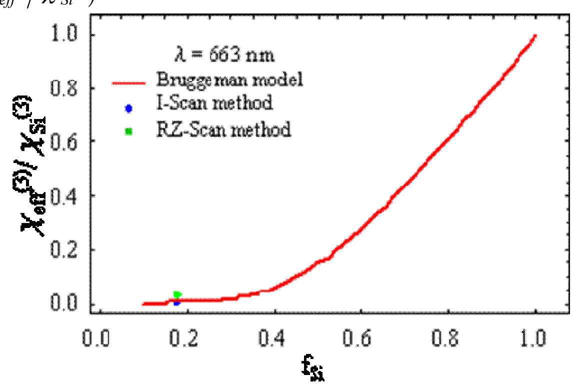

Fig. 11. Theoretical predictions of $\chi_{eff}^{(3)}$ given by our Eq. (7) and the experimental results obtained with I-Scan and RZ-Scan for our np-Si sample, with f_{Si} = 0.18

By I-Scan, we obtained a value of $\left(\chi_{eff}^{(3)} / \chi_{Si}^{(3)}\right) = 6.7 \times 10^{-3}$, which is in a reasonable agreement with simplified Bruggeman prediction. By RZ-Scan, we have obtained $\left|\chi_{eff}^{(3)} / \chi_{Si}^{(3)}\right| = 3.03 \times 10^{-2}$. There are several reasons, for which the I-Scan method gives better results than RZ-Scan method in the measurement of the third-order optical nonlinearities. First, the sample is never passing through the focal plane, where it is exposed to a large irradiance (like in the case of RZ-Scan method). Second, the total exposure time is reduced and the thermal effects and other sample distortions are smaller. Third, the same area of the sample is illuminated during the experimental measurements.

4. Conclusions

This study brings contributions to the simplification of Bruggeman model for nano-composites, applies the simplified relations in the study of linear and nonlinear optical properties of the np-Si samples and experimentally confirms the validity of these relations. We have experimentally determined, for np-Si samples with f_{Si} = 0.18, the effective refractive index, n_{eff} = 1.303, and the ratio between effective third-order nonlinear susceptibilities of np-Si and bulk Si, respectively, $\left(\chi_{eff}^{(3)} / \chi_{Si}^{(3)}\right) = 6.7 \times 10^{-3}$ (with I-Scan), which is in a reasonable good agreement with the prediction of the simplified Bruggeman formalism.

Acknowledgements

The authors acknowledge the financial support of the COST Action MP0702, Core Project – PN 09/39.01.02 and PNCDI II project- No. 12111/2008.

References

[1] Z. Gaburro, N. Daldosso, L. Pavesi, „Porous Silicon”, in Enciclopedia of Condensed Matter Physics, edited by F. Bassani, J. Liedl, P. Wyder (Elsevier Ltd.) (2005)
[2] P. Bettotti, M. Cazzanelli, L. Dal Negro, B. Danese, Z. Gaburro, C. J. Oton, G. Vijaya Prakash, L. Pavesi, J. Phys.:Condens. Matter **14**, 8253 (2002)
[3] F. Z. Henari, K. Morgenstern, W. J. Blau, V. A. Karavanskii, V.S. Dneprovskii, Appl. Phys. Lett. **67** (3), 323 (1995)
[4] S. Vijayalakshmi, M. A. George, H. Grebel, Appl. Phys. Lett. **70** (6), 708 (1997)
[5] S. Vijayalakshmi, F. Shen, H. Grebel, Appl. Phys. Lett. **71** (23), 3332 (1997)
[6] S. Lettieri, P. Maddalena, J. Appl. Phys. **91**(8), 5564 (2002)
[7] K. S. Bindra, Opt. Commun. **246**, 421 (2005)
[8] R.W. Boyd, R.J. Gehr, G.L. Fischer, J.E. Sipe, Pure Appl. Opt. **5**, 505 (1996)
[9] R. J. Gehr, G. L. Fischer, R.W. Boyd, J. Opt. Soc. Am. B **14**(9), 2310 (1997)
[10] B. Taheri, H. Liu, B. Jassemnejad, D. Appling, R. C. Powell, J.J. Song, Appl. Phys. Lett. **68**(10), 1317 (1996)
[11] M. Martinelli, S. Bian, J.R. Leite, R. J. Horowicz, Appl. Phys. Lett. **72**(12), 1427 (1998)
[12] M. Martinelli, L. Gomes, R. J. Horowicz, Appl. Opt. **39**(12), 1427 (1998)
[13] A. Petris, F. Pettazzi, E. Fazio, C. Peroz, Y. Chen, V. I. Vlad, M. Bertolotti, Proc. SPIE **6785**, 67850P (2007)
[14] L.T. Canham, Appl. Phys. Lett. **57**(10), 1046 (1990).
[15] M. L. Ciurea, V. Iancu, V. Teodorescu, L. Nistor, M. G. Blanchin, J. Electrochem. Soc., **146**, 3516 (1999)
[16] I. Inanc, A. Kurt, A. Serpenguzel, J. Carey, E. Mazur, „Photoluminescence in nanocrystalline silicon”, PhOREMOST Workshop “Advances in nanophotonics", Istanbul (2007)
[17] A. Kux, M. Ben Chorin, Phys. Rev. B **51**(24), 17535 (1995)
[18] P. D. J. Calcott, “Experimental estimates of porous silicon bandgap, Properties of Porous Silicon”, Edited by L. Canham, EMIS Datareviews Series n. 18, INSPEC Publ., London, p. 203 (1997)
[19] S. Lettieri, O. Fiore, P. Maddalena, D. Ninno, G. Di Francia, V. La Ferrara, Opt. Commun. **168**, 383 (1999)

*Corresponding author: tatiana.bazaru@inflpr.ro